APPENDIX AVAILABLE ON REQUEST

Research Report 147

Atmospheric Transformation of Diesel Emissions

Barbara Zielinska et al.

Appendix B. Detailed Results From NOx Denuder Development and Characterization

Citation for document:
Zielinska B, Samy S, McDonald JD, Seagrave J. 2010. Atmospheric Transformation of Diesel Emissions. HEI Research Report 147. Health Effects Institute, Boston, MA.

Correspondence may be addressed to Dr. Barbara Zielinska, Division of Atmospheric Sciences, Desert Research Institute, 2215 Raggio Parkway, Reno, Nevada 89512-1905.

Although this document was produced with partial funding by the United States Environmental Protection Agency under Assistance Award CR–83234701 to the Health Effects Institute, it has not been subjected to the Agency's peer and administrative review and therefore may not necessarily reflect the views of the Agency, and no official endorsement by it should be inferred. The contents of this document also have not been reviewed by private party institutions, including those that support the Health Effects Institute; therefore, it may not reflect the views or policies of these parties, and no endorsement by them should be inferred.

This document was reviewed by the HEI Health Review Committee
but did not undergo the HEI scientific editing and production process.

APPENDIX B

B. DETAILED RESULTS FROM NOx DENUDER DEVELOPMENT AND CHARACTERIZATION

1. Development

The cordierite honeycomb denuder used in the summer 2005 campaign allowed for sectional transport of the denuder and simple on-site assembly. Figure 1 displays the assembled honeycomb denuder and a coated section. The ceramic cylinders are 5.7 inches in diameter and 3 inches in length (Applied Ceramics, Inc.), with sixteen 0.19 inch internal diameter channels per square inch. Up to 12 Applied Ceramic pieces were soaked in a nearly-saturated aqueous solution of cobalt nitrate hexahydrate, $CoN_2O_6 \bullet 6H_2O$. Between one and two kilograms of this compound were taken up by 12 ceramic pieces in the initial soaking process. The ceramic pieces were then baked in a temperature-controlled oven at 400° C for at least 12 hours.

Just prior to the summer 2005 campaign, eight sections of Applied Ceramics material were subjected to a particle transmission test using a light-duty diesel engine as the aerosol source at DRI. An extraction line was inserted into the tailpipe of a delivery van powered by a 2003 Mercedes-Benz 154 horsepower diesel engine equipped with a catalytic converter. The engine was allowed to run at idle until the temperature gauge stabilized at an indicated temperature of 190°C. Particle size distribution data were obtained upstream and downstream from the ceramic sections using a DRI Scanning Mobility Particle Size (SMPS) spectrometer. Particle losses in the denuder were estimated by averaging two or more upstream and downstream spectra whenever possible, then taking the difference. The losses were usually greatest for particles as small as 10-50 nm in diameter, for which as many as 70% were removed by the denuder. Losses were usually least for those with diameters near 100 nm, while loss percentages rise as high as 50% for particles with diameters near 400 nm. Losses at the small-diameter ends of the spectra are attributable to diffusion, while those at the large-diameter ends are attributable to impaction.

Due to limitations on resources and time the experiments prior to the summer 2005 campaign (at DRI) were conducted with a polyvinylchloride (PVC) denuder housing. The losses of electrically charged particles to the walls of the PVC housing and (electrically insulating) coated ceramic pieces used in this experiment were expected but very difficult to predict in advance of the experiments. Following the diesel exhaust test, black bands of particle deposits were observed on the inner walls of the PVC housing around the perimeter of each ceramic piece. These bands corresponded to small aerosol flows that by-passed the honeycomb sections and passed through the very small clearances around the perimeter of each piece. A noticeable black deposit was found on the upstream face of the ceramic piece closest to the inlet, suggesting that the flow formed an inlet jet that then led to some impaction particle loss on the first ceramic piece.

The final version of the housing was stainless steel (Figure 1), which reduces electrostatic effects. Due to the indicated impaction zone on the upstream face of the ceramic section closest to the inlet (mentioned above), an approximate 58cm unpacked section (pre-chamber) was included at the denuder inlet. Heating of the honeycomb denuder was necessary (80˚ C) to prevent the condensation of water inside the denuder body.

Our initial development experiments for a new, improved NOx denuder, following the summer 2005 campaign utilized a simple four-channel annular design(fall 2005), constructed with stainless steel mesh (Figure 2). The length of each channel is 39cm, with a channel diameter of 2.5cm. An additional 15 cm pre-chamber was constructed to establish laminar flow of effluent, prior to the channel entrances. Packing of absorbent material on the outside of the main interior channels allows for efficient transport and replacement of the packing material (or regeneration). Once effluent flow is established, gaseous diffusion through the mesh apertures (~1mm) allows for efficient removal of NO_x. Channel pathways were left completely open (line-of-site), to reduce particulate loss due to impaction.

1.1 Absorbent Material Chemistry

The potential NO_x storage capacity of cobalt oxide has been documented in the past (Vijay et al., 2005; Haneda et al., 2004; Saathoff et al., 2003). Yet, addition of barium (Ba) to the cobalt oxide has been shown to enhance the storage capacity by spillover of NO_2 to the Ba-NO_x storage sites (in conjunction with NO attack of the Co site). Experiment #1 and #2 (described below) were performed in the fall of 2005 to establish a NOx removal efficiency value for pure cobalt oxide and the Barium/Cobalt oxide combination. Experiment #3 was conducted to establish a parameter for the optimal absorbent depth for NO removal efficiency.

1.1.1 Substrate Selection

Use of an aluminum oxide (Al_2O_3) substrate in preparation of the NO_x absorbent has been shown to be effective and beneficial for absorbent stability (Hendershot, 2004). After evaluation of several types of alumina (aluminum oxide), it was obvious that the material would not be practical to prepare, handle, and regenerate. Further investigations led to a firebrick prerequisite material, with an industrial reference name of *GROG*. *GROG* is composed of silca (~50%), alumina (~%40), iron oxide (~2%), titanium oxide (~2%), and several other earth metal oxides (sodium, potassium, etc…). It can be purchased at varying size ranges (diameters), and is readily available through the firebrick production industry. Figure 3 displays the *GROG* in both pre-coated, and coated (with Cobalt Oxide) forms. Filling the exterior section (around the empty 4-channels) of the denuder body with the Co/Ba impregnated *GROG*, several experiments were conducted. Abbreviated results follow.

1.1.1.1 Experiment #1: an initial evaluation

The NO/air mixture (400ppm certified standard) flow rate through the miniature denuder was set utilizing a calibrated mass flow meter. A Fourier Transform Infrared Spectrometer (FTIR) allowed for the detection of the output NO concentrations from the denuder body. Figure 4 shows the assembled miniature denuder with heating elments during experimentation.

An average flow of 3.35 LPM (EUPHORE experiment flow is ~54 times greater) was established throughout the first experimental stage. Evaluation of residence time for the 768 cubic centimeter(cc), four-channel denuder, indicates a duration of approximately 13.7 seconds. The denuder was heated to 100^{o} C (a pre-chamber was utilized to preheat the source gas), and the 400ppm NO source regularly reconnected directly to the instrument to assure appropriate response. The source gas standard was also run through the heated sample line and connected directly to the instrument to test for sample line losses. Pure nitrogen gas was utilized as a zeroing agent, and all responses were within instrumental tolerances (<15%, with a typical response of 2ppm for pure nitrogen).

At the above mentioned conditions, 3.67×10^{-5} moles/minute of NO entered the denuder. NO removal efficiency remained >90% for approximately 80 minutes. Figure 5 graphically displays the FTIR response, with a best-fit linear approximation. At ~120 minutes, a leveling off at approximately >70% removal efficiency occurred. After this a calibration level and baseline check was performed, and the denuder was reconnected for an additional 15 minutes. A consistent ~120 ppm plateau was observed for this time period. This response remained consistent with the data displayed in Figure 5 (>70% removal efficiency). A 2^{nd} order polynomial trend-line evaluation of the data in Figure 4, followed by a simple integration, resulted in a 10.7% total NO breakthrough for the entire 121 minutes. A total of 4 mmoles of NO were captured by the coated *GROG* (only 121 minutes included).

1.1.1.1a Denuder Desorption (Regenerative) Capabilities

The impact of effluent/source gas temperature upon NO absorption efficiency of cobalt oxide coated *GROG* is not well understood. A temperature ramp experiment was conducted to confirm (and perhaps reveal) some suspicions about the influence of temperature on the NO storage capacity of the cobalt oxide coating. Note that this experiment was performed with non-saturated cobalt oxide *GROG* (with respect to NO_x). An initial check of the NO removal efficiency (before beginning the temp. ramp), confirmed the >70% removal efficiency observed at the conclusion of experiment #1 (see above). This was the same material from the previous experiment, left inside the denuder with no disturbance (to mimic in-field conditions). A 4 LPM flow of pure nitrogen through the denuder channels, with a 50 C initial temperature, produced a ~10ppm FTIR response. A temperature ramp was performed with an approximate hold time of 15 minutes for each 25 degree step.

Figure 6 represents one of the temperature ramp/FTIR response beginning at 50 C (0-30 minutes), followed by 100 C (30 minutes), 125 C (45-50 minutes), 150 C (65 minutes), and 175 C (80 minutes). The coinciding desorption peaks in Figure 6 indicate a clear correlation and dependence of denuder/effluent temperature on storage capacity. Visible effluent became apparent at temperatures above 150 C. It should be noted that each step in the temperature ramp did result in slight "overshoot" or higher actual temperature readings (e.g. setting of 125 C resulted in an actual reading of 134 C). The highest recorded temperature for this experiment was 183 C. Following a cool down of the denuder (~80 C), a 10 minute check of immediate removal efficiency was confirmed (>90%). These results are important for application issues, which should be addressed when dealing with a heated effluent source/transfer-line. Operating the denuder system at 100 C will likely reduce the removal efficiency, relative to lower temperature scenarios.

1.1.1.2 Experiment #2: Barium/Cobalt Chemistry

Addition of Barium (Ba) to NOx catalysts has been shown to increase the NO_x storage capacity of the material (Vijay et al., 2005, Hendershot et al., 2004). Spillover of NO_x into the barium storage sites, via cobalt storage sites, is the suggested mechanism for a six-fold increase in material storage capacity (see above mentioned references for detailed description). These results prompted an investigation of the Ba/Co oxide chemistry to determine if an increase in storage capacity equates to a more efficient bonding mechanism, which may increase the overall removal efficiency. Any enhancement of our absorbent material may help to achieve the >90% NO_x removal threshold, which we seek to achieve for the EUPHORE experiments. A 2.6:1 weight/weight ratio of Ba:Co was utilized to coat *GROG* (263 grams of Ba/101 grams of Co).

Figure 7 is a graphical depiction of the FTIR response for the first Ba/Co experiment. The linear character of the break through of NO, over the first 40 minutes does indicate a lack of capturing enhancement. The average flow rate was set near 3.55 LPM, and the FTIR response for the 400ppm standard 435ppm. Figure 8 displays the next day absorption capability of the same Ba/Co coated *GROG*. The >90% removal efficiency was only achieved for approximately 60 minutes (400 ppm standard response was at 454ppm). The peak near 45 minutes was the result of an increase of standard flow to 9.29 LPM. This indicates the importance of residence time when evaluating the open cylindrical denuder configuration. Past adjustment of flow (with pure Co *GROG*), produced similar results. The denuder was heated overnight, and the regenerative capability was evaluated with a new 540ppm NO standard. The material did efficiently regenerate, and the >90% removal threshold was reestablished.

1.1.1.3 Experiment #3: GROG depth impacts on absorptive capabilities.

This experiment was an attempt to increase our understanding of the depth penetration of the gaseous NO into the cobalt oxide coated *GROG (Co/GROG).* A sealed stainless steel chamber was constructed with a dispersive inlet/outlet system and an adjustable base to maintain consistent headspace volumes. Two specific depths, weights, and volumes of *Co/GROG* were established for this experiment. First, a depth of 0.25-0.50cm was established in the base of the chamber. This corresponded to a total weight of 635 gram, and a volume of 500 mL. Then the experiment was repeated with a 0.5-0.75cm *Co/GROG* depth (1157 grams, 900mL). The average *Co/GROG* density was 1.28 g/mL. Figure 9 shows the FTIR response for the two different depths. The three different slopes in this figure represent three different flow rates (i.e. chamber residence times). A 4.7 LPM flow was established for the first slope, followed by a 2.4 LPM and 1.2 LPM flow. The dip in response indicates that the *Co/GROG* NO capacity was not at saturation, and given more time, the material was still absorbing the 339ppm NO standard mixture at increased levels.

This experiment does not only highlight the importance of flow rate (i.e. effluent residence time), but also indicates a necessity to maintain a minimal depth tolerance when constructing a parallel channel diffusion denuder. Figure 10 and 11 are an evaluation of the 4.7 LPM slope for the two different *Co/GROG* depths (first slope in Figure 9). Note the variance in the slope values of the two best-fit regression equations. Depth experiment #2 (greater depth), produced a 1.20 slope, while the initial depth experiment #1 (less depth) resulted in a 1.70 slope value. This indicates that with identical effluent residence times, the *Co/GROG* depth did significantly alter the removal efficiency.

Figure 12 displays the three different slope values for each depth and flow rate. It is important to note that the reduction in flow, corresponds to an increase in effluent residence time. The fact that the greater depth produces a consistently lower slope value suggests that diffusive penetration of effluent gas is occurring. In addition, the greatest variance of slope did occur at the slowest flow rate (longest residence time), also pointing to a greater ability for the material to absorb NO when present at similar surface area (i.e. chamber area), but greater depth. Finally, the similar slope produced between the 4.7 LPM versus 2.4 LPM with the lower depth (1.701 versus 1.687), indicates a "depth threshold" that was not established with the deeper material. Specifically, the deeper material had a rather significant variance in slope between all three flows ($R^2 > 0.99$), pointing to a capacity that had not reached a gaseous diffusive penetration limit ("depth threshold"). This is a crucial variable for the appropriate design of a scaled up NOx denuder.

1.1.2 Summary

The capacity of the cobalt oxide coating is sufficient for efficient removal of NOx, and the *GROG* appears to be an appropriate substrate material. Addition of barium to the

Co/GROG does not appear to significantly enhance the capturing capabilities of the absorbent. The regenerative properties of the *Co/GROG* appears to be sufficient for multiple use scenarios. The use of oxygen rich air (30-40% in both regeneration and production), appears to enhance the efficiency of the *Co/GROG*. This impact on efficiency was most visible when pure nitrogen was utilized in the regeneration procedure (i.e. versus oxygen rich air) Even though time and resource limitations only allowed a qualitative evaluation, we hypothesize that the more oxidative environment enhances the production and regeneration of the material. In addition, diffusion depth penetration of effluent gas needs to be considered for optimal denuder performance.

1.2 Scaled up Denuder, the EUPHORE Experiments

A stainless steel (304) perforated tube with 24 gauge (~ 1mm) apertures was utilized for the denuder channels. This spiral seamed tubing is 167 cm in length (66”), and has a 2.54cm (1”) outer diameter. The channels are straight cylinders. Figure 13 is a sketch of the scaled up external denuder dimensions. The internal channel configuration allows for a minimum of 1.5 cm of *Co/GROG* space between all channels. The denuder was built in April 2006 and shipped to Valencia, Spain, on May 1, 2006. Figure 14 shows the scaled up NOx denuder partially assembled, with the first channel alignment plate and internal channels visible (right panel) and the position of the channels inside the main denuder body (left panel). Following this assembly stage, the *Co/GROG* is utilized to fill in the volume, between the channels, and the black caps (on top of the perforated tubes) are removed before the denuder is closed and prepared for exhaust introduction. An external view of the denuder mounted on the wheeled base (left panel) with the effluent entrance elbow visible (arrow), and denuder inside a specially constructed transportation crate (right panel) is provided in Figure 15. For a view of the valve-denuder-chamber setup, during diesel injection and the denuder heating jackets see Figure 16.

1.2.1 Denuder Performance

Initial conditions for a subset of experimental runs performed at the EUPHORE chamber in May-June 2006 with and without the NOx denuder can be viewed in Table 1. The runs are listed in chronological order (05/26/06 to 06/13/06), and the NOx denuder was regenerated between runs by heating to 400 ˚C with an established air/oxygen mixture flow (20-30 LPM), for 3-4 hours. Cooling the denuder to 80 ˚C required an overnight duration (12–14 hours), which allowed for the next diesel exhaust (DE) injection with efficient NOx removal. Degradation of the denuder performance after repeated regenerations was not apparent. Based on the data shown in Table 1, we can conclude that the newly designed denuder removes NOx very efficiently. For example, the NOx concentrations in the chamber were in the range of 9-50 ppb for 20–30 minute total injection times. Without the NOx denuder (for equivalent times), these concentrations would be in the 2-3 ppm range. Thus, the denuder achieved the 95% removal efficiency goal, with a sufficient storage capacity. Some perturbation of particle distributions (median particle diameter increased from ~60nm to ~90nm), with the denuder in-line,

was observed (Table 1). The increased injection and transit times may be partially responsible for this shift (i.e. additional connective plumbing allowing more time for the small particles to coagulate). Figure 17 displays the aging particle profiles for an experiment with (Dd06s_2 on 05/31/06), and without the denuder (D06s_3 on 06/13/06).

The DPM concentration in the injected effluent stream was reduced due to NOx denuder usage (both honeycomb in 2005 and diffusion in 2006). Without the NOx diffusion denuder in-line, we obtained an average mass concentration of 10.08ug/L (+/-10%) for the summer 2006 campaign (4 experiments total). In contrast, with the NOx diffusion denuder in-line, we obtained 5.05ug/L (+/-28%, total of 9 experiments). However, the DPM concentration depends on the engine loading and small differences in the loading over the course of the diesel exhaust injection can make a significant difference for DPM values. The dynamometer loading tends to decrease over the course of an injection, so a longer injection time results in a lower than predicted particle concentration. Figure 18 displays the decrease in torque (Nm) applied by the dynamometer for a summer 2005 experiment. To confirm this influence, we examined the injection effluent mass concentration for summer 2005 experiments with and without accelerating engine cycles. It was found that experiments with cycling resulted in a 7.9ug/L (+/- 16%) DPM concentration, while those without cycling were reduced to 5.5ug/L (+/- 6%). This represents an approximate 30% reduction in DPM for the 2005 experiments conducted without an acceleration cycle. The longer injection times in 2006 also displayed similar trends, and may partially explain the lower DPM concentrations with the denuder in-line.

Since the injection valve system at EUPHORE depends upon a positive pressure split flow regime, addition of the denuder (including transfer lines) does reduce the injection flow rate into the chamber (i.e. creates additional back pressure at the split valve). Assuming a conservation of NOx and an approximate 204.5M3 chamber volume, a flow can be calculated by using the engine-out (Horiba) and chamber NOx mixing ratios immediately following injection. In this fashion, an approximate 129 LPM (+/- 4%) flow rate was calculated using the values from the 4 DE, dark experiments in 2006 (without denuder). Direct mass flow measurements during several 2006 experiments indicated a reduction of injection flow to 50 LPM with the denuder in-line. This lower injection flow rate does partially explain the required extension of injection times to achieve similar chamber mass loadings, and the above mentioned engine loading trends.

Table 2 displays the averaged concentrations in ng/mgEC for summer 2006 dark experiments with (Dd06s_1 on 05/30/06, Dd06s_2 on 05/31/06) and without denuder (D06s_2 on 05/26/06, D06s_3 on 06/13/06) for several different compound groups. Looking at the percent difference values (%Difference = [(Without Denuder – With Denuder)/Without Denuder] multiplied by 100) it is apparent that the general compound removal trend suggests a gas-phase selectivity. For example a comparison of naphthalene (predominately gas-phase) to pyrene, which was almost exclusively found in particle-phase, indicates a significant difference in relative removal with the denuder in-line. The sum (gas- + particle-phase) of PAHs removed in 2006 was 44%, while total sum of alkanes appear to be less perturbed by denudation (-14%). Hopanes were detected in the

particle-phase of the chamber samples, and displayed a 5% difference without the denuder.

While no injection in summer 2005 were performed without the denuder housing in-line, a few injections were made without the ceramic sections installed. In other words, the injections were performed with only the transfer lines and denuder body in-line. Comparing the mass concentrations for these experiments, it is clear that the ceramic sections did remove a significant fraction of the particle mass (~29%). Table 2 includes the PAHs sum (gas- and particle-phase) for this summer 2005 dark experiment, and has been classified as "With Denuder." The significant difference with the summer 2006 dark experiment "With Denuder" PAHs sum (over 6 times the 2005 value) is difficult to attribute to differences in denuder technology (i.e. honeycomb vs. diffusion), due to variability in loading, engine age, and slight variability in engine operating conditions (DiLorenzo et al., 1991).

FTIR data indicates the emission of nitrous acid (HONO) in experiments without the denuder (i.e. high NOx conditions), in the range of 30-50ppb (+/-10ppb). Figure 19 displays the HONO concentrations for the two dark without denuder experiments (D06s_2 on 05/26/06, D06s_3 on 06/13/06). HONO was below detection limits in experiments with the denuder (Dd06s_1 on 05/30/06, Dd06s_2 on 05/31/06), but is thought to be in the low ppb range (from 2005 LOPAP data). The formation of NPAHs in experiments without the denuder appears to be greatly enhanced (Table 2), but may be partially due to sampling artifacts involving PAH nitration on filters (or XAD cartridges) during sampling. Gas-phase NPAH concentrations are approximately an order of magnitude higher for high NOx experiments versus low NOx, while the particle-phase production is nearly two times the low NOx experiments. The most abundant NPAHs include 1-nitronaphthalene and 1-nitropyrene, which is consistent with past studies of primary diesel emissions (Zielinska et al., 2004).

1.2.2 Further Work

Modification of the denuder filling routine will enhance the ease-of-use issues faced with this initial application. A maximum experimental flow and NO concentration threshold should be established with the scaled up denuder to reduce exhaust residence time and reduce particle losses due to settling. However, particle losses due to impaction need to be kept in mind throughout this process to avoid further perturbation. SMPS monitoring of a stable particle source pre- and post-denuder will further characterize the profile perturbation.

List of Tables

List of Figures

Table 1. Initial conditions for a subset of experiments with and without NOx denuder from summer 2006

Run type	*NOx Denuder usage*	*Engine-out NOx(ppm)*	*Time of DE injection (min)*	*Chamber NOx (ppm)*	*DPM (µg/m3)*	*Median Diameter (nm)*	*Mean Diameter (nm)*
DE, dark	***No***	***430***	***6***	***1.7***	***33***	***62***	***71***
DE, dark	***No***	***410***	***10***	***2.6***	***60***	***61***	***69***
DE, dark	***Yes***	***390***	***20***	***0.009***	***30***	***75***	***84***
DE, light	***Yes***	***415***	***27***	***0.050***	***54***	***88***	***100***
DE,light+OH	***Yes***	***400***	***15+10+10***	***0.025***	***37***	***87***	***96***
DE,light+OH	***Yes***	***410***	***17+7+6***	***0.025***	***30***	***91***	***100***
DE, light	***Yes***	***371***	***20+10***	***0.024***	***42***	***94***	***103***
DE, light +tol	***Yes***	***363***	***20+10***	***0.034***	***39***	***93***	***102***
DE, dark	***No***	***398***	***10***	***2.5***	***66***	***65***	***74***

Note: The experiments are chronologically ordered and the table lists the experimental type, engine-out NOx concentrations, time over which diesel exhaust (DE) was introduced into the chamber, NOx concentrations in the chamber, initial diesel particulate matter (DPM) concentrations in the chamber measured by SMPS (assuming a 1 g/cm^3 particle density), and the initial mean and median particle diameter.

Table 2. Average chamber concentrations (ng/mg EC) of selected compounds with and without NOx denuder.

Compound/Group	With Denuder[a]	Without Denuder[b]	%Difference[c]
naphthalene	**49425**	**126869**	**61%**
pyrene	**138**	**131**	**-5%**
PAHs sum	**162694**	**291079**	**44%**
PAHs sum 2005	**25250**	**N/A**	**N/A**
n-alkanes	**872625**	**659542**	**-32%**
n-alkyl-cyclohexanes	**71125**	**89792**	**20%**
iso-alkanes	**119838**	**178509**	**32%**
alkanes total sum	**1063588**	**927842**	**-14%**
hopanes	**756**	**800**	**5%**
steranes	**375**	**629**	**40%**
1-nitro-naphthalene	**305**	**1697**	**82%**
1-nitro-pyrene	**66**	**107**	**38%**
NPAHs sum(particle)	**248**	**463**	**46%**
NPAHs sum(gas)	**258**	**2292**	**88%**

[a] Values with denuder are averaged for Dd06s_1(05/30/06) and Dd06s_2(05/31/06). [b] Values without denuder are averaged for D06s_2(05/26/06) and D06s_3(06/13/06). [c] %Difference = [(Without Denuder – With Denuder)/Without Denuder] multiplied by 100. N/A= Data Not Available. Note: list of all group compounds are included in main report, “particle” implies particle-phase totals, “gas” implies gas-phase totals, and “sum” implies gas- and particle-phase totals. All values are for summer 2006 campaign, unless stated otherwise.

Figure 1. Cordierite honeycomb NOx denuder used in summer 2005. Left panel: NOx denuder installed in EUPHOR facility; right panel: honeycomb structure of one ceramic piece, coated with cobalt oxide.

Figure 2. 4-Channel miniature annular denuder.

Figure 3. GROG before (left) and after (right) coating with cobalt oxide.

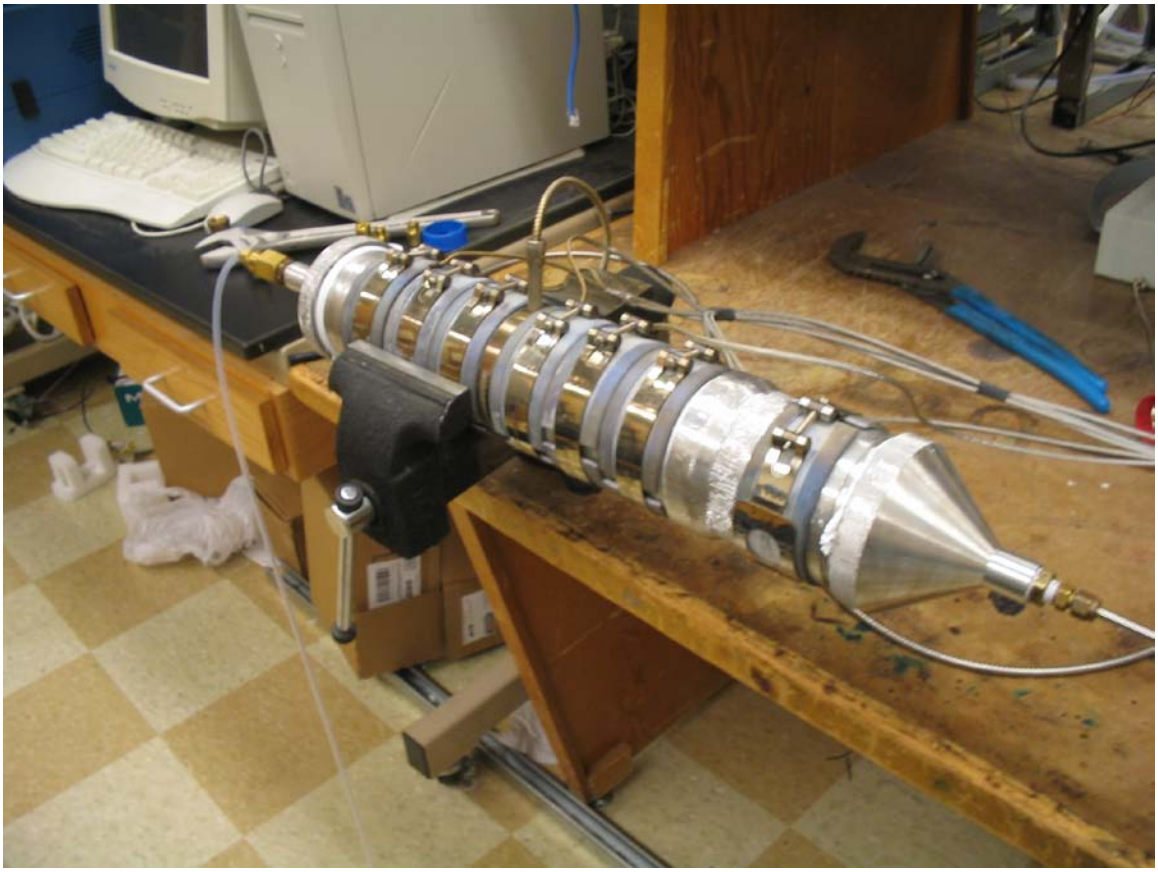

Figure 4. Miniature NOx denuder, w/heaters, used in the initial stage of experiments.

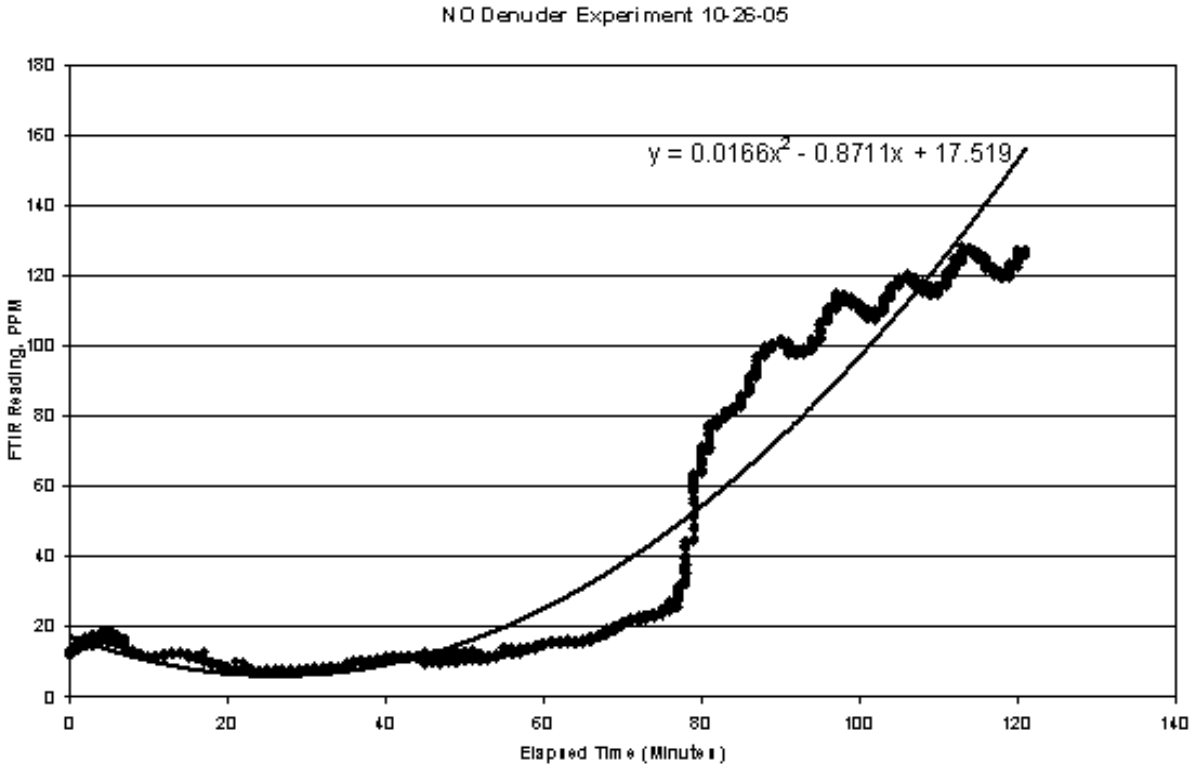

Figure 5. NO removal by the miniature NOx denuder. Experimental conditions: 400ppm NO standard FTIR reading with denuder removed from flow path = 455ppm, Nitrogen zero = 1-2ppm.

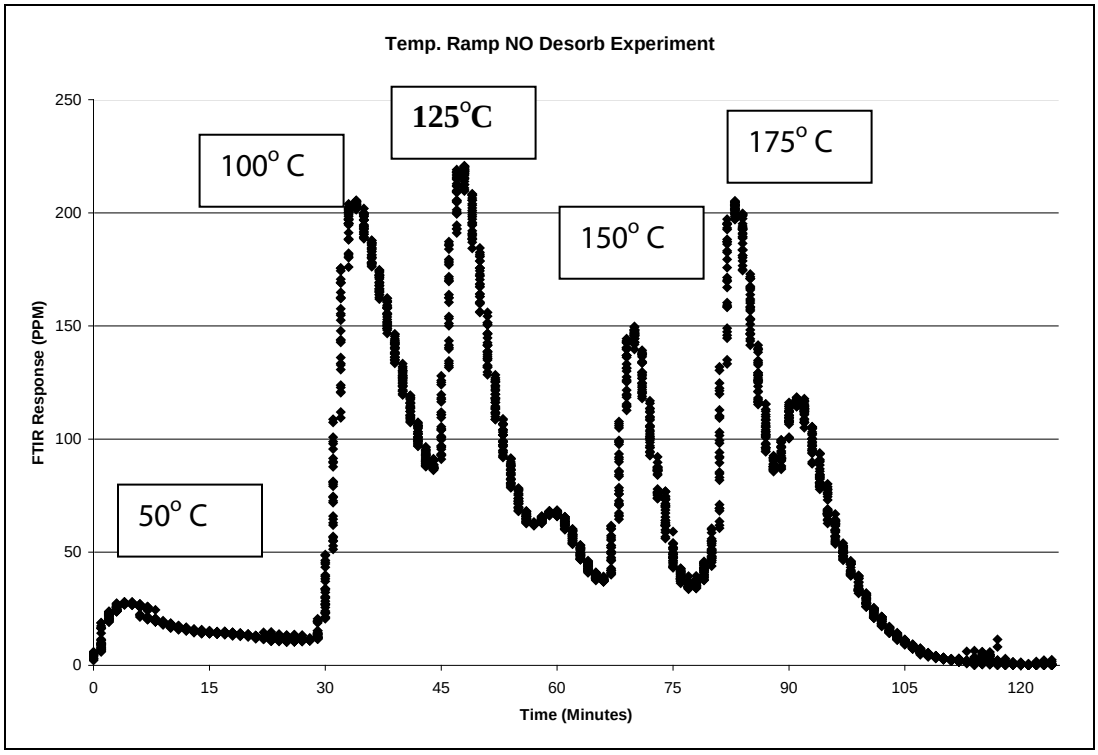

Figure 6. Final temperature ramp experiment, w/associated temperature settings for each NO desorption peak.

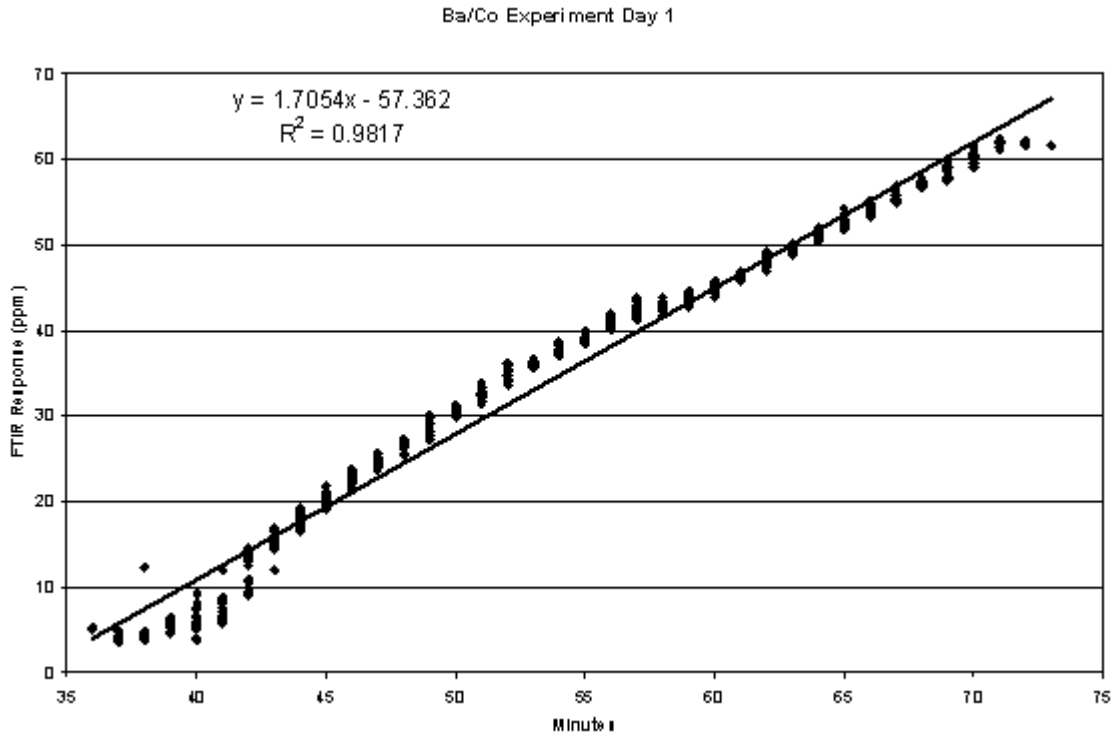

Figure 7. Initial Ba/Co coated GROG experiment displaying linear breakthrough.

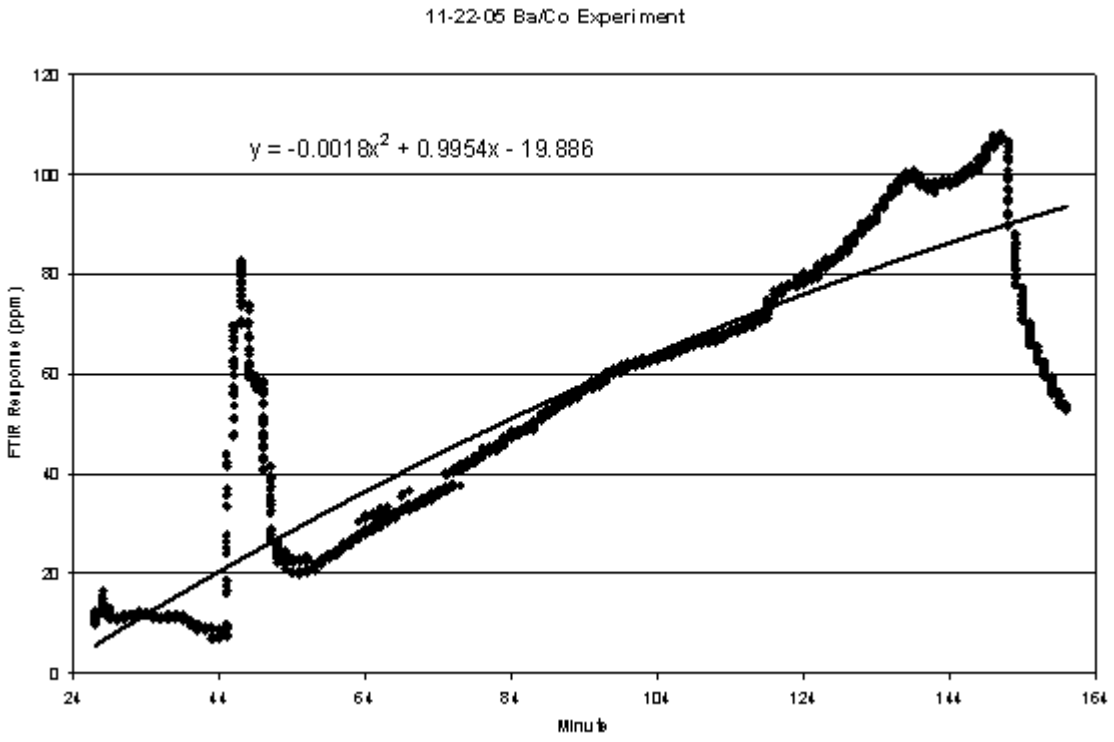

Figure 8. Final Ba/Co experiment, 44min peak is associated with elevated flow.

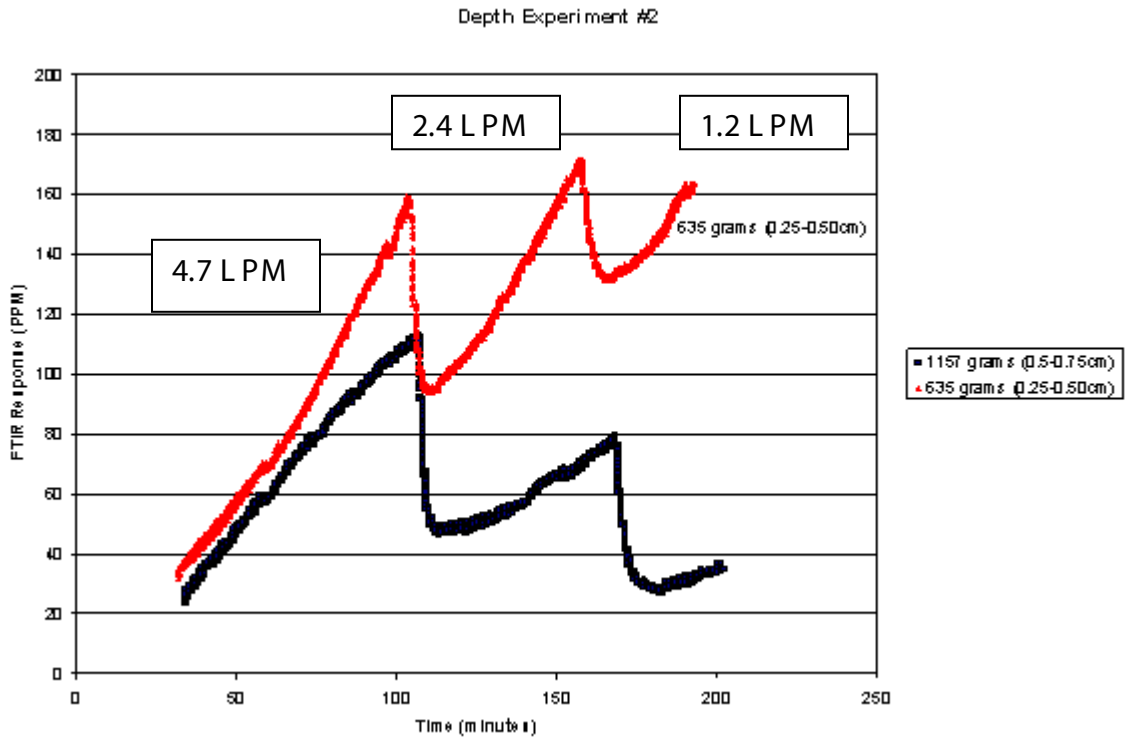

Figure 9. NO breakthrough profiles at two depths, w/flow variance for each breakthrough slope.

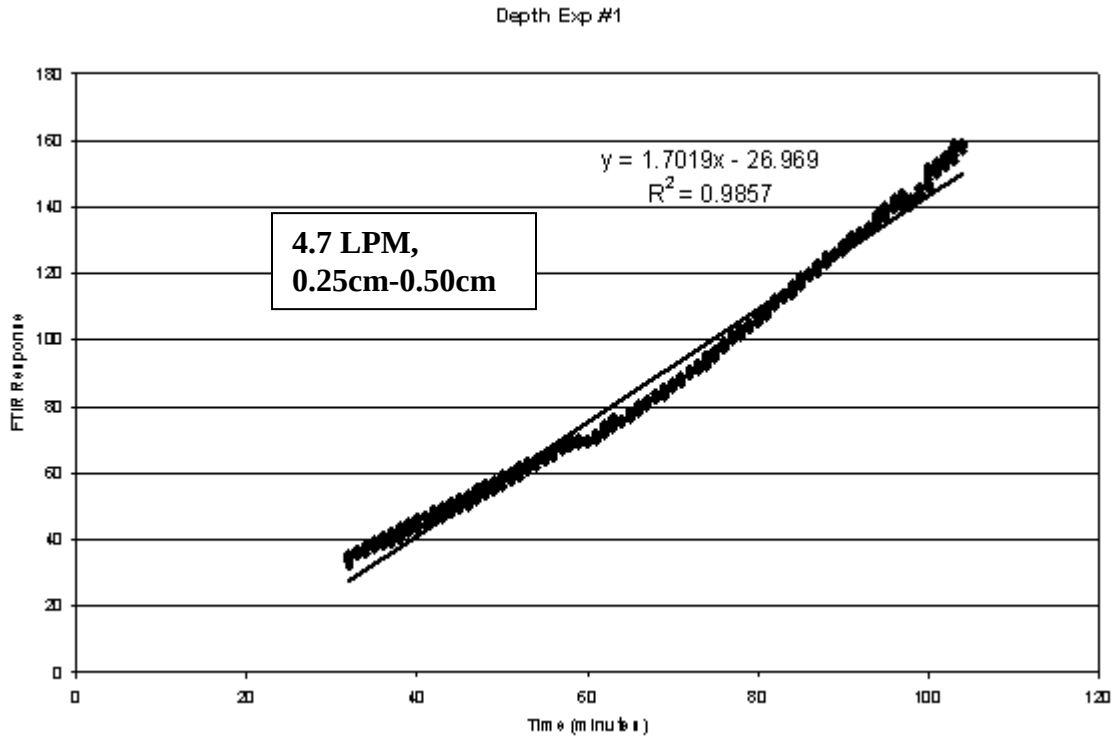

Figure 10. Breakthrough profile for first flow rate, w/least Co/GROG depth

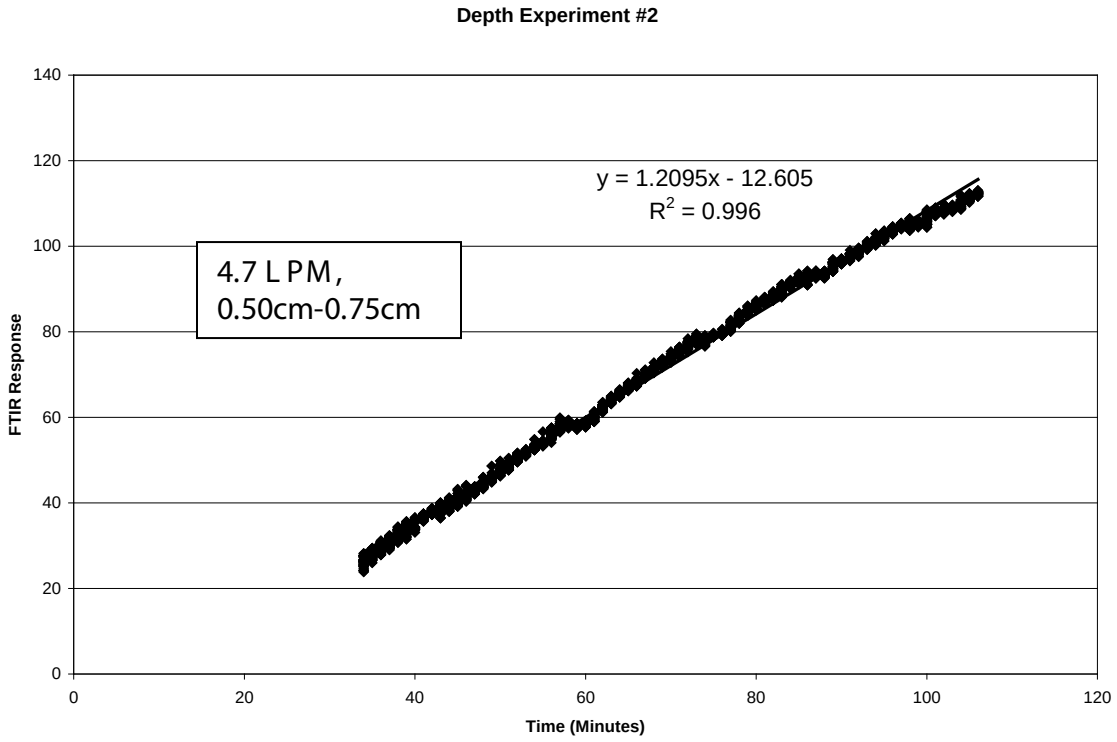

Figure 11. Breakthrough profile for first flow, w/greater Co/GROG depth.

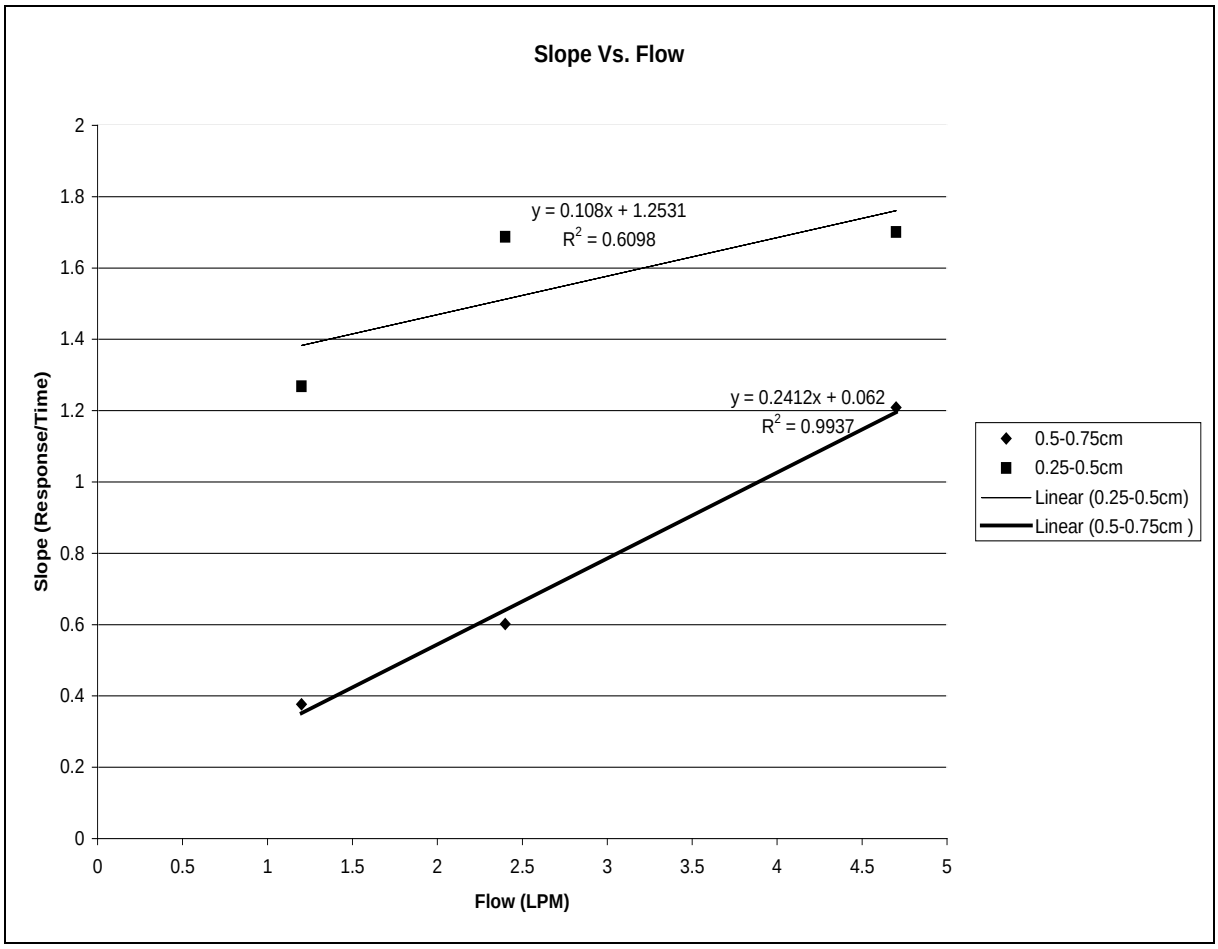

Figure 12 . Graphical representation of breakthrough slope values (at two depths).

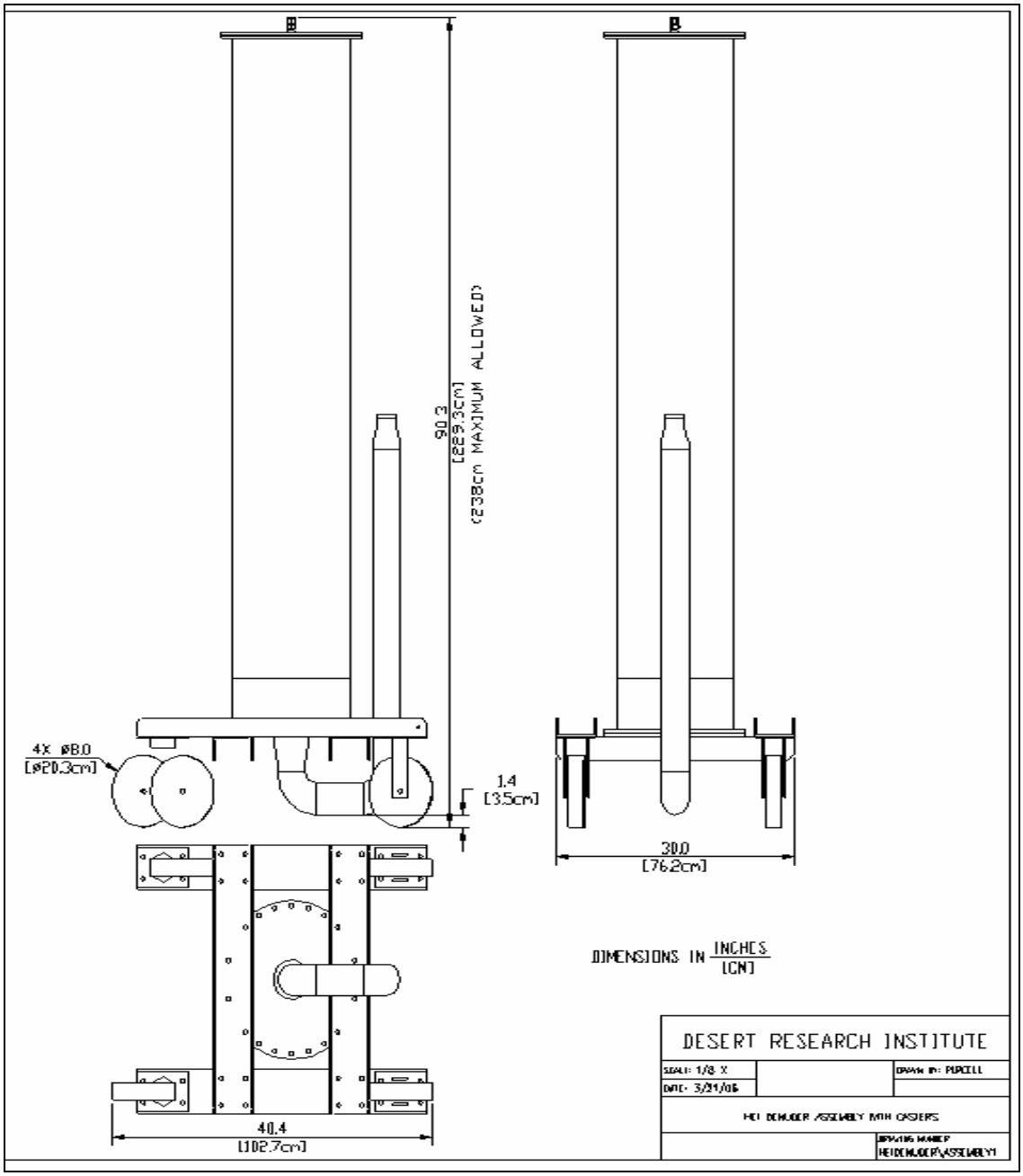

Figure 13. Sketch of the NOx denuder.

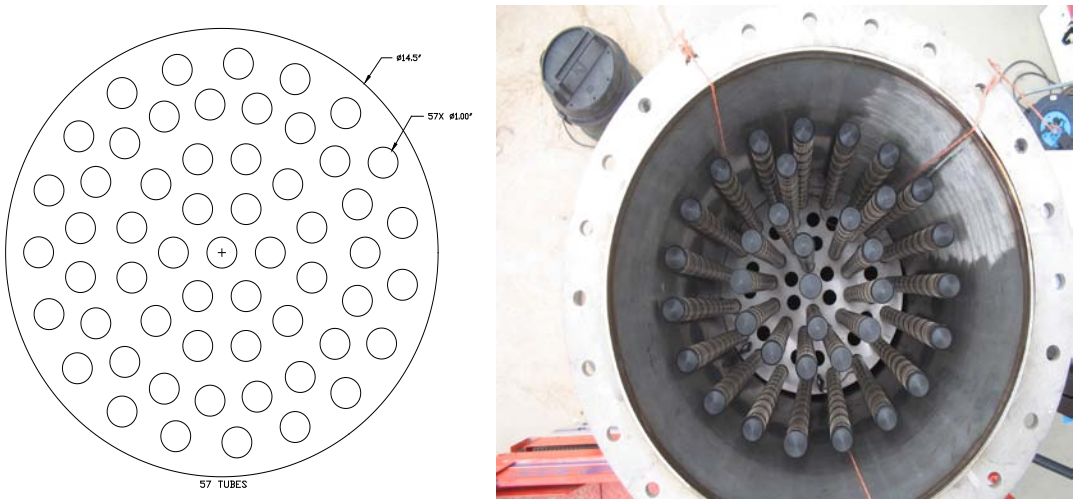

Figure 14 . Internal channel configuration (left panel), and partially assembled annular diffusion denuder viewed from above with alignment plate and internal channels visible.

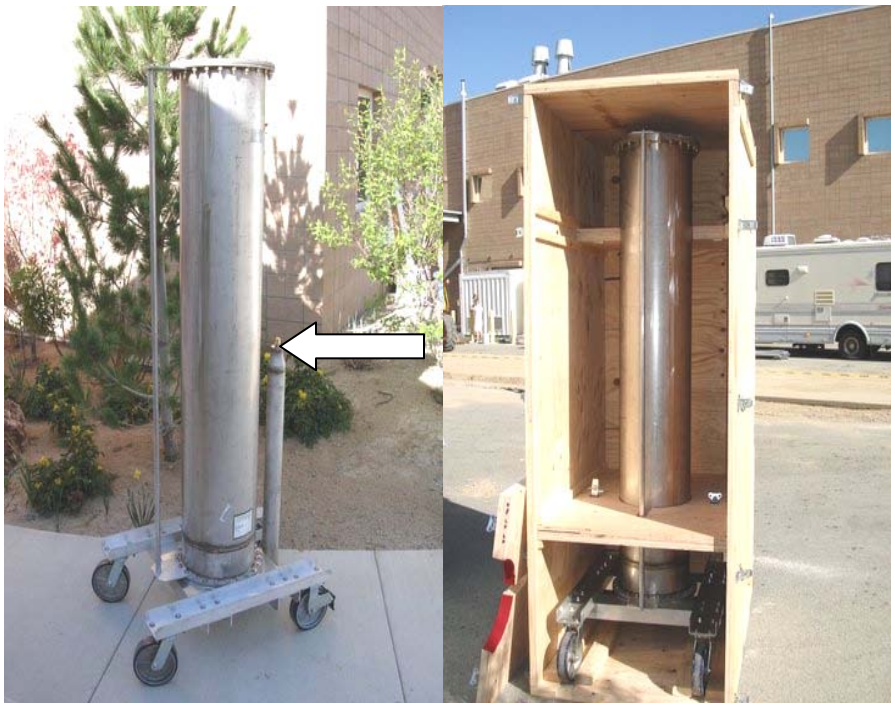

Figure 15. Denuder mounted on wheeled base (left panel) with effluent entrance elbow visible (arrow), and denuder inside specially constructed transportation crate (right panel).

Figure 16. Setup of valve-denuder-chamber effluent tubing during injection, arrow indicates chamber entrance line (left panel), and denuder with heating mantel (right panel), secured below the chamber.

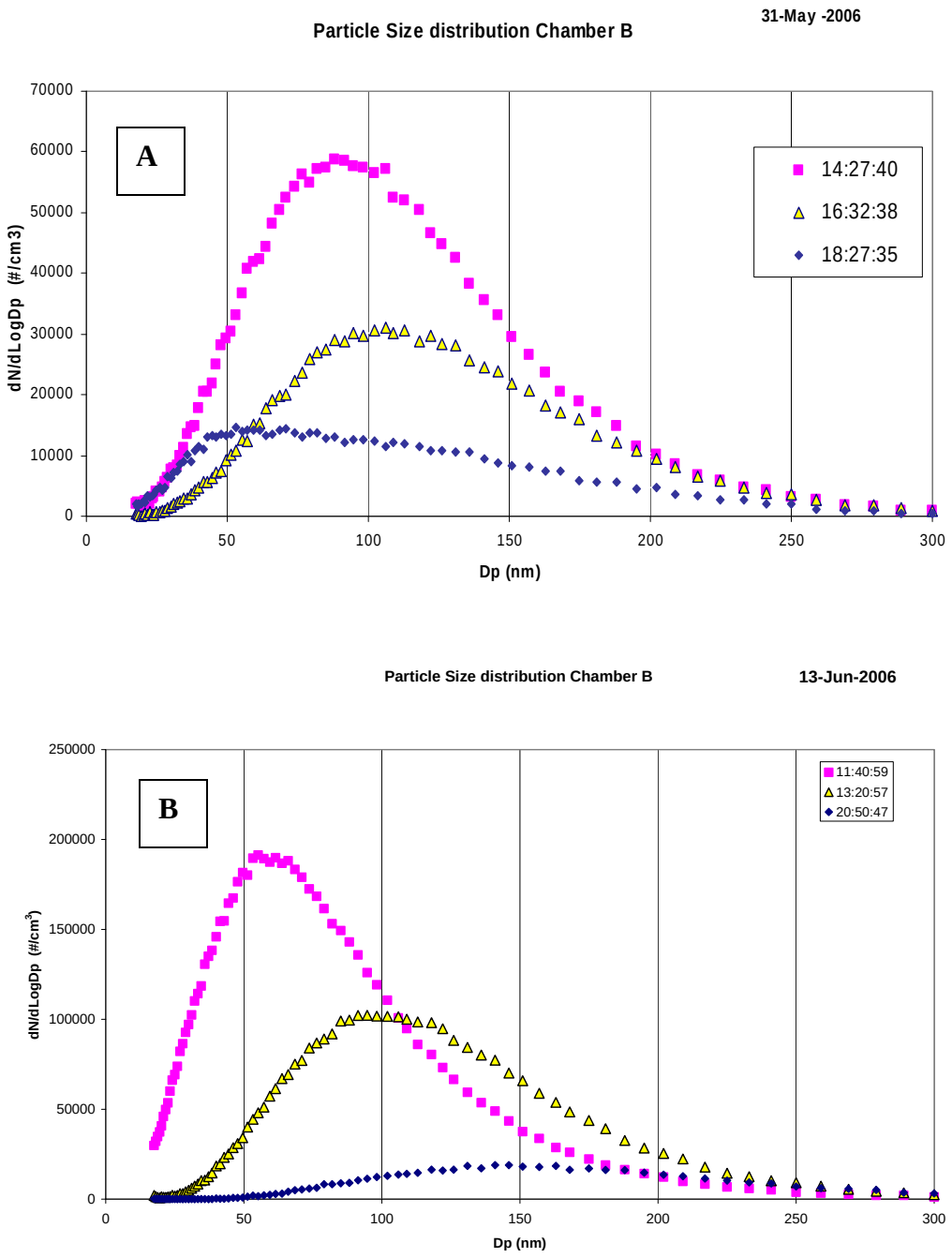

Figure 17. Particle size and number concentration distribution during diesel exhaust aging in EUPHORE chamber in the dark in summer 2006; (A) with NOx denuder (initial DPM concentration 30 µg/m3); (B) without NOx denuder (initial DPM 65 µg/m3). The legend indicates particles right after diesel exhaust injection (▪), after two hours of aging (▲) and after 4 hrs of aging (◆).

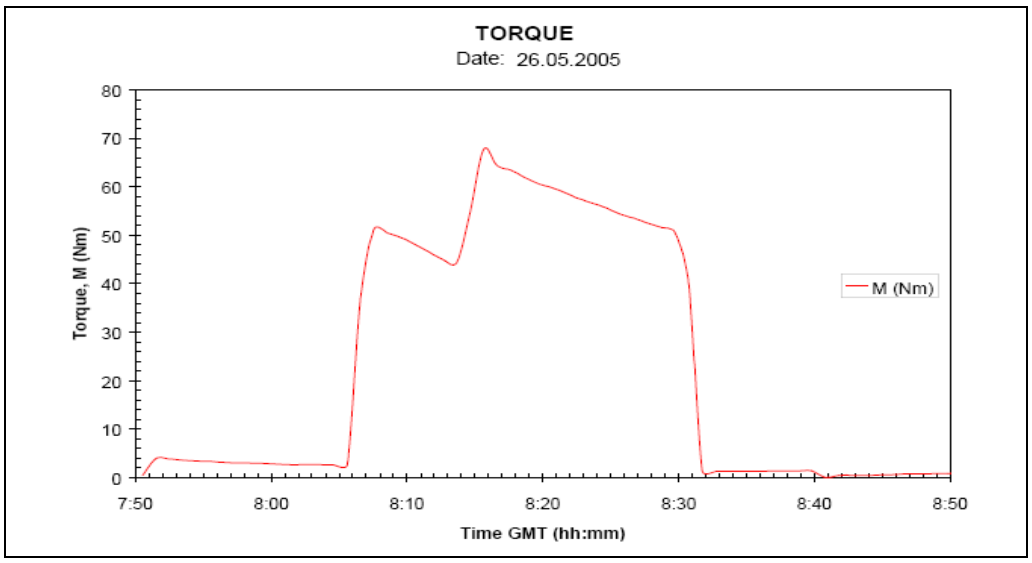

Figure 18. Graphical display of torque in Newton meters (Nm) during diesel injection at 8:20-8:30 on May 26, 2005.

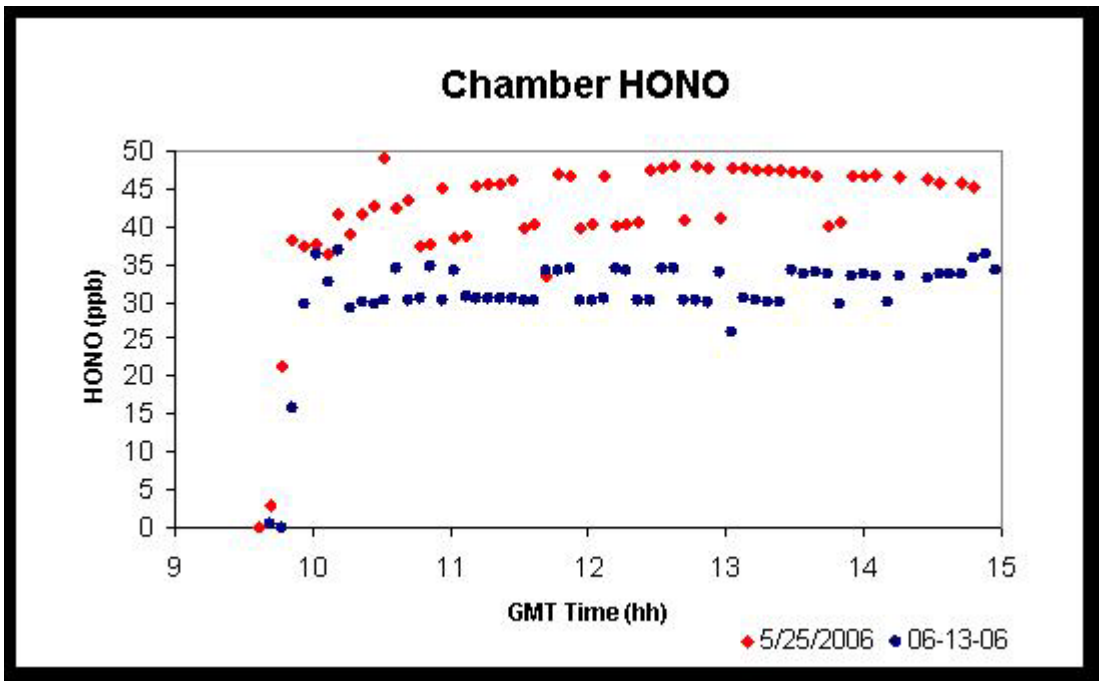

Figure 19. Dilution corrected HONO values for two dark without denuder experiments.

References

Ammann, M., 2001: *Radiochim. Acta*, **89**, 831-838.

Arens, F., L. Gutzwiller, U. Baltensperger, H. W. Gaggeler and M. Amman, 2001: *Environ. Sci. Technol*., **35**, 2191-2199.

Braman, R.S. and M.A. de la Centera, 1986: *Anal. Chem*., **58**, 1537-1541.

DiLorenzo, A., Polletta, A., Ciccioli, P., Brancaleoni, E., and A. Cecinato, 1991. *Polynuclear Aromatic Hydrocarbons*, Battelle Press, Columbus, 239-258.

Haneda, M., Tsuboi, G., Nagao, Y., Kintaichi, Y., Hamada, H., 2004. *Catalysis Letters*, **97** (3-4), pg. 145.

Hendershot, R.J., Rogers, W.B. Snively, C.M., Ogunnaike B.A., Lauterbach, J., 2004. *Catalysis Today*, **98**, pg. 375.

Rogers, C.F, J.C. Sagebiel, B. Zielinska, W.P. Arnott, E.M. Fujita, J.D. McDonald, J.B. Griffin, K. Kelly, D. Overacker, D. Wagner, J.S. Lighty, A. Sarofim, and G. Palmer, 2003: *Aerosol Sci. Technol.*, **37**, 355-368.

Saathof, H., O. Moehler, U. Schurath, S. Kamm, B. Dippel, and D. Mihelcic, 2003. *J. Aerosol Sci.*, **34**, 1277-1296.

Vijay, R., Hendershot, R.J., Rivera-Jimenez, S.M., Rogers, W.B., Feist, B.J., Snively C.M., Lauterbach, J., 2005. *Catalysis Communications*, **6**, pg. 167.

Zielinska, B., Sagebiel, J., McDonald, J.D., Whitney, K., and D.R. Lawson, 2004. *J. Air & Waste Manage. Assoc.*, **54**, 1138-1150.